J. Ocean Univ. China (Oceanic and Coastal Sea Research)
DOI 10.1007/s11802-016-2674-9
ISSN 1672-5182, 2016 15 (2): 241-246
http://www.ouc.edu.cn/xbywb/
E-mail:xbywb@ouc.edu.cn

Depth Classification of Underwater Targets Based on Complex Acoustic Intensity of Normal Modes

YANG Guang[1)], YIN Jingwei[1), *], YU Yun[2)], and SHI Zhenhua[3)]

1) *Acoustic Science and Technology Laboratory*, *College of Underwater Acoustic Engineering*, *Harbin Engineering University*, *Harbin* 150001, *P. R. China*
2) *Naval Academy of Armament*, *Beijing* 100161, *P. R. China*
3) *Department of Mechanical Engineering*, *Massachusetts Institute of Technology*, *Boston Mit* 77, *USA*

(Received May 19, 2014; revised October 17, 2014; accepted November 30, 2015)

Abstract In order to solve the problem of depth classification of the underwater target in a very low frequency acoustic field, the active component of cross spectra of particle pressure and horizontal velocity (ACCSPPHV) is adopted to distinguish the surface vessel and the underwater target. According to the effective depth of a Pekeris waveguide, the placing depth forecasting equations of passive vertical double vector hydrophones are proposed. Numerical examples show that when the sum of depths of two hydrophones is the effective depth, the sign distribution of ACCSPPHV has nothing to do with horizontal distance; in addition, the sum of the first critical surface and the second critical surface is equal to the effective depth. By setting the first critical surface less than the difference between the effective water depth and the actual water depth, that is, the second critical surface is greater than the actual depth, the three positive and negative regions of the whole ocean volume are equivalent to two positive and negative regions and therefore the depth classification of the underwater target is obtained. Besides, when the 20 m water depth is taken as the first critical surface in the simulation of underwater targets (40 Hz, 50 Hz, and 60 Hz respectively), the effectiveness of the algorithm and the correctness of relevant conclusions are verified, and the analysis of the corresponding forecasting performance is conducted.

Key words the placing depth forecasting equations; the effective depth; depth classification; Pekeris waveguide

1 Introduction

There are about 150 countries with coastlines around the world. At present, it is difficult to detect adversary underwater targets by conventional means, which could seriously threaten the safety of these countries. Due to the acoustic features of an underwater target in a very low frequency range (10–100 Hz), this paper adopts the ACCSPPHV to conduct the depth classification of low-noise targets, that is, the binary decision of surface targets and underwater targets, which has bright prospects of potential applications in a coast warning system, such as Vertical Double Towed Lines Array, Aeronautical Underwater Acoustic Buoy, *etc*.

Many algorithms have been used to detect and localize underwater targets. Josso *et al.* (2010) investigated underwater targets' motion detection and estimation. Baggenstoss (2011) carried out localization research of multiple interfering sperm whales using time difference. Dosso and Wilmut (2011) researched multiple underwater targets' localization. Michalopoulou *et al.* (2011) investigated the passive tracking algorithm based on particle filtering. Wiggins *et al.* (2012) researched the underwater targets' tracking using a multichannel autonomous acoustic recorder. Dubreuil *et al.* (2013) researched underwater target's detection taking advantage of imaging polarimetry and correlation techniques. Diamant *et al.* (2014) did the underwater acoustic localization research using LOS and NLOS algorithms. Gerstein and Gerstein (2014) did some research on sound localization in shallow waters. Forero (2014) investigated broadband underwater target's localization by multitask learning.

In this paper, the Pekeris waveguide model and ACCSPPHV of passive vertical double vector hydrophones are used to divide the whole ocean volume into two parts, which solves the depth classification problem of underwater targets. Based on our prior research (Hui *et al.*, 2008; Yu *et al.*, 2008, 2009), research is conducted in implementing the placing depth forecasting equations based on ACCSPPHV of vertical double vector hydrophones.

2 Depth Classification Theory and Placing Forecasting Equations

An underwater target usually radiates strong line spectra below 100 Hz, and therefore, the Pekeris Model is employed in this paper. The waveguide diagram is shown

* Corresponding author. E-mail: edit231@163.com

in Fig.1.

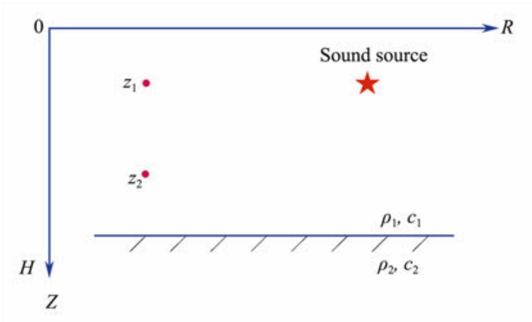

Fig.1 Pekeris waveguide.

The particle sound pressure equation is given as (Liu, 2010),

$$p(r,z_0,z)=2\pi\omega\rho_1\sum_n \sin(\beta_{1n}z)F(z_0,\varepsilon_n)H_0^{(1)}(\varepsilon_n r)$$

$$\approx e^{-j\frac{\pi}{4}}\sqrt{\frac{8\pi}{r}}\omega\rho_1\sum_n\sqrt{\frac{1}{\varepsilon_n}}\sin(\beta_{1n}z)F(z_0,\varepsilon_n)e^{j\varepsilon_n r}, \quad (1)$$

where

$$F(z_0,\varepsilon_n)=\frac{\beta_{1n}\sin(\beta_{1n}z_0)}{\beta_{1n}H-\sin(\beta_{1n}H)\cos(\beta_{1n}H)-b^2\tan(\beta_{1n}H)\sin^2(\beta_{1n}H)},$$

n represents the order of normal modes,

$$\beta_{1n}=\sqrt{k_1^2-\varepsilon_n^2}, \quad b=\rho_1/\rho_2, \quad k_i=\omega/c_i \ (i=1,2),$$

ρ_1 and ρ_2 are the densities of seawater and seafloor, respectively, z_0 is the depth of underwater target, z is the placing depth of hydrophone, r is the horizontal distance between z_0 and z, ε_n is the eigenvalue of the nth normal mode, which is the root of the following eigenvalue equation

$$x\cos x-jb\sqrt{x^2-\sigma^2}\sin x=0, \quad (2)$$

where

$$x=\beta_1 H, \quad \sigma^2=(k_1^2-k_2^2)H^2.$$

Every normal mode corresponds to one cut-off frequency f_n, namely, when the frequency of a sound source $f<f_n$, the nth normal mode can not be motivated by the sound source. f_n can be expressed as (Liu, 2010),

$$f_n=\frac{(n-\frac{1}{2})c_1c_2}{2H\sqrt{c_2^2-c_1^2}}. \quad (3)$$

The relationship between particle velocity and sound pressure is (Brekhovskikh and Lysanov, 2003)

$$\rho\frac{\partial v}{\partial t}=-\nabla p, \quad (4)$$

where v contains the time factor. Thus, the above equation can be written as

$$v=\frac{1}{j\omega\rho}\nabla p=\frac{1}{j\omega\rho}[\frac{\partial p}{\partial r}i+\frac{\partial p}{\partial z}k]. \quad (5)$$

Substituting Eq. (1) into Eq. (5), the horizontal and vertical components of the particle velocity are given respectively as

$$v_r\approx e^{-j\frac{\pi}{4}}\sqrt{\frac{8\pi}{r}}\sum_n\sqrt{\varepsilon_n}\sin(\beta_{1n}z)F(z_0,\varepsilon_n)e^{j\varepsilon_n r}, \quad (6)$$

and

$$v_z\approx -je^{-j\frac{\pi}{4}}\sqrt{\frac{8\pi}{r}}\sum_n\sqrt{\frac{1}{\varepsilon_n}}\beta_{1n}\cos(\beta_{1n}z)F(z_0,\varepsilon_n)e^{j\varepsilon_n r}. \quad (7)$$

According to Eq. (1) and Eq. (6), the cross spectra of particle sound pressure and horizontal velocity of vertical double vector hydrophones can be obtained from its active component part as

$$I_r=pv_r^*$$

$$=\frac{8\pi\omega\rho_1}{r}\left(\sum_n\sin(\beta_{1n}z_1)\sin(\beta_{1n}z_2)F^2(z_0,\varepsilon_n)+\sum_{n,n\neq m}\sum_m\sqrt{\frac{\varepsilon_m}{\varepsilon_n}}\sin(\beta_{1n}z_1)\sin(\beta_{1m}z_2)F(z_0,\varepsilon_n)F(z_0,\varepsilon_m)e^{j[(\varepsilon_n-\varepsilon_m)r]}\right), \quad (8)$$

and the vital ACCSPPHV can be obtained as

$$I_{rA}=$$

$$\frac{8\pi\omega\rho_1}{r}\left(\sum_n\sin(\beta_{1n}z_1)\sin(\beta_{1n}z_2)F^2(z_0,\varepsilon_n)+\sum_{n,n\neq m}\sum_m\sqrt{\frac{\varepsilon_m}{\varepsilon_n}}\sin(\beta_{1n}z_1)\sin(\beta_{1m}z_2)F(z_0,\varepsilon_n)F(z_0,\varepsilon_m)\cos[(\varepsilon_n-\varepsilon_m)r]\right). \quad (9)$$

When there are only two normal modes in underwater acoustic field, that is, only the first two normal modes are considered in this paper, Eq. (9) can be expanded and simplified for analytical convenience:

$$I_{rA}\approx\sin(\beta_{11}z_1)\sin(\beta_{11}z_2)F^2(z_0,\varepsilon_1)+\sin(\beta_{12}z_1)\sin(\beta_{12}z_2)F^2(z_0,\varepsilon_2)+$$

$$\sin(\beta_{11}z_1)\sin(\beta_{12}z_2)F(z_0,\varepsilon_1)F(z_0,\varepsilon_2)\cos[(\varepsilon_1-\varepsilon_2)r]+\sin(\beta_{12}z_1)\sin(\beta_{11}z_2)F(z_0,\varepsilon_2)F(z_0,\varepsilon_1)\cos[(\varepsilon_2-\varepsilon_1)r]. \quad (10)$$

According to Eq. (10), when receiver points z_1 and z_2 are fixed and the sign of ACCSPPHV is kept unchanged with distance r, it is easy to get

$$\sin(\beta_{11}z_1)\sin(\beta_{12}z_2)F(z_0,\varepsilon_1)F(z_0,\varepsilon_2)\cos[(\varepsilon_1-\varepsilon_2)r]+$$
$$\sin(\beta_{12}z_1)\sin(\beta_{11}z_2)F(z_0,\varepsilon_2)F(z_0,\varepsilon_1)\cos[(\varepsilon_2-\varepsilon_1)r]=0. \quad (11)$$

The Pekeris model can be equivalent to the environment where the effective water depth is absolutely soft, and the expression of the effective water depth is (Buchingham and Giddens, 2006)

$$H_e=H\left[1+\frac{1}{bk_1H\sin(\alpha_c)}\right], \quad (12)$$

where H_e is the effective water depth, H represents the actual water depth, b is the density ratio of seawater to seafloor, k_1 is the wave number in seawater, and $\alpha_c=\cos^{-1}(c_1/c_2)$, representing the critical grazing angle. Then, Eq. (11) can be converted to

$$\sin(\frac{\pi}{H_e}z_1)\sin(\frac{2\pi}{H_e}z_2)+\sin(\frac{2\pi}{H_e}z_1)\sin(\frac{\pi}{H_e}z_2)=0. \quad (13)$$

Because $\pi z_1/H_e$, $\pi z_2/H_e\in[0, \pi)$ in Eq. (13), a critical conclusion can be drawn

$$z_1+z_2=H_e. \quad (14)$$

Therefore, only if the summation of the placing depths of two hydrophones equals the effective water depth, the cross spectra sign of the particle sound pressure and the horizontal velocities of the hydrophones are irrelevant to the horizontal distance r. Thus, the depth classification of the underwater target can be made based on this law. When Eq. (14) is met, Eq. (10) can be changed to

$$I_{rA}\approx\sin(\frac{\pi}{H_e}z_1)\sin(\frac{\pi}{H_e}z_2)\sin^2(\frac{\pi}{H_e}z_0)+\sin(\frac{2\pi}{H_e}z_1)\sin(\frac{2\pi}{H_e}z_2)\sin^2(\frac{2\pi}{H_e}z_0)$$
$$\approx\sin(\frac{\pi}{H_e}z_1)\sin(\frac{\pi}{H_e}z_2)\sin^2(\frac{\pi}{H_e}z_0)\times[1-16\cos^2(\frac{\pi}{H_e}z_1)\cos^2(\frac{\pi}{H_e}z_0)]. \quad (15)$$

Assuming

$$F=[1-16\cos^2(\pi z_1/H_e)\cos^2(\pi z_0/H_e)],$$

the sign of I_{rA} is decided by F. Due to $\pi z_0/H_e\in[0, \pi)$, $\cos^2(\pi z_0/H_e)$ is a monotonic decreasing function when $z_0\in[0, H_e/2]$ and a monotone increasing function when $z_0\in[H_e/2, H_e]$, *i.e.*, the function is symmetric with respect to $H_e/2$. For a nonzero F, we can get

$$\begin{cases}F>0,\ z_0\in(h_1,\ h_2)\\ F<0,\ z_0\in(0,\ h_1)\cup(h_2,\ H_e)\end{cases}, \quad (16)$$

$$h_1+h_2=H_e, \quad (17)$$

where h_1 represents $\frac{H_e}{\pi}\arccos\sqrt{\frac{1}{16\cos^2(\frac{\pi}{H_e}z_1)}}$, and h_2 represents $\frac{H_e}{\pi}\arccos\left[-\sqrt{\frac{1}{16\cos^2(\frac{\pi}{H_e}z_1)}}\right]$.

From Eq. (16), the whole ocean volume can be divided into three parts, negative value−positive value−negative value, within the effective water depth H_e, and the summation of the two critical surfaces is H_e. When the first critical surface h_1 is less than H_e-H, the second critical surface h_2 is greater than the actual water depth H. At this time, the second negative value region is invalid. By setting the first critical surface h_1, the theoretical forecasting equations on the placing depth of the two hydrophones can be written as

$$z_1=\frac{H_e}{\pi}\arccos\sqrt{\frac{1}{16\cos^2(\frac{\pi}{H_e}h_1)}}, \quad (18)$$

$$z_2=\frac{H_e}{\pi}\arccos\left[-\sqrt{\frac{1}{16\cos^2(\frac{\pi}{H_e}h_1)}}\right]. \quad (19)$$

3 Simulation

For single-frequency acoustic waves from a point sound source, the water depth H=100 m, the particle velocity c_1=1500 m s^{-1}, the seabed medium sound velocity c_2=1570 m s^{-1}, ρ_1=1.025 g cm^{-3}, and ρ_2=1.766 g cm^{-3}. According to Eq. (3), the cut-off frequencies of the first five normal modes are shown in Table 1. On the basis of Eq. (12), H_e can be obtained as shown in Table 2. When the sound source frequency $38.1008<f<63.5013$, only the first two normal modes need to be considered.

Table 1 The cut-off frequencies of the first five normal modes

n	f_n (Hz)
1	12.70
2	38.10
3	63.50
4	88.90
5	114.30

Table 2 Effective water depths of 40 Hz, 50 Hz, and 60 Hz

f (Hz)	H_e (m)
40	134.83
50	127.86
60	123.22

Take 40 Hz, 50 Hz, and 60 Hz as examples, white represents the positive value, and blue represents the negative value.

1) The frequency of the underwater target is 40 Hz. If setting h_1=20 m as the first critical surface, z_1=55.24 m and z_2=79.59 m can be obtained according to Eqs. (18)–(19). The vertical double hydrophones are placed at the depth of z_1=50.7 m and z_2=80.1 m respectively, and Fig. 2(a) shows the results by Eq. (9). Furthermore, the summation of placing depths is 130.8 m. If putting the vertical double hydrophones at z_1=43 m, z_2=88 m, the summation is 131 m and the results are shown in Fig.2(b). The critical surfaces are h_1=38 m, h_2=93 m, the summation of which is 131 m. All the three summations are close to the theoretical effective water depth 134.83 m.

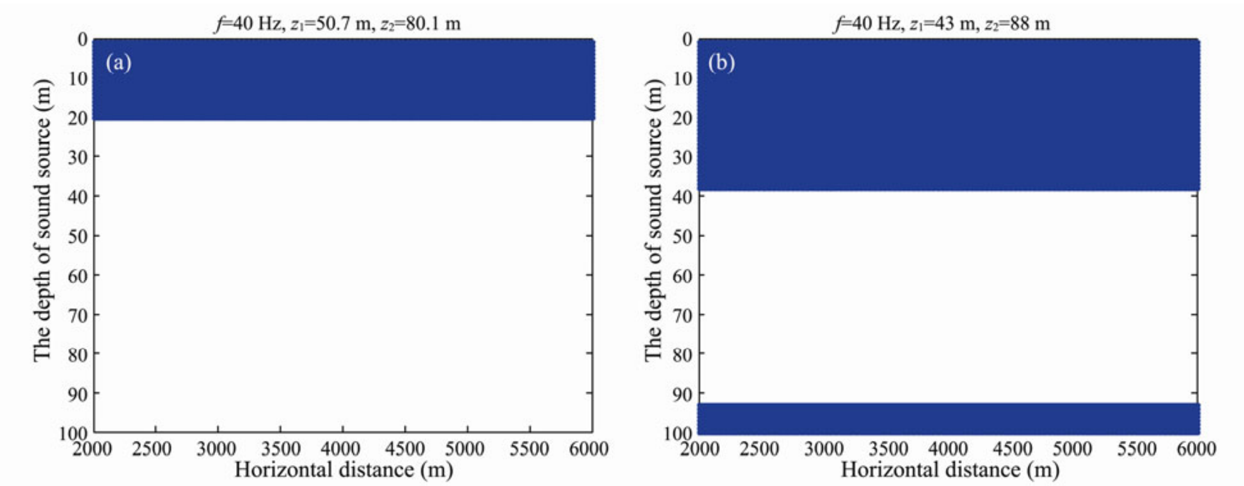

Fig.2 The sign change of ACCSPPHV with f=40 Hz.

2) The target frequency is 50 Hz. Based on Eqs. (18)–(19), setting h_1=20 m as the first critical surface, z_1=52.23 m and z_2=75.63 m can be obtained. If the vertical double hydrophones are placed at z_1=50.9 m, z_2=73.1 m, respectively, the summation of placing depths is 124 m. Fig.3(a) shows the results obtained by Eq. (9) and Fig.3(b) by placing the vertical double hydrophones at z_1=37.9 m, z_2=86.3 m with the placing depth summation of 124.2 m. When the critical surfaces are h_1=44 m and h_2=80 m, the summation of h_1 and h_2 is 124 m. All the three summations well match the corresponding theoretical effective water depth of 127.86 m.

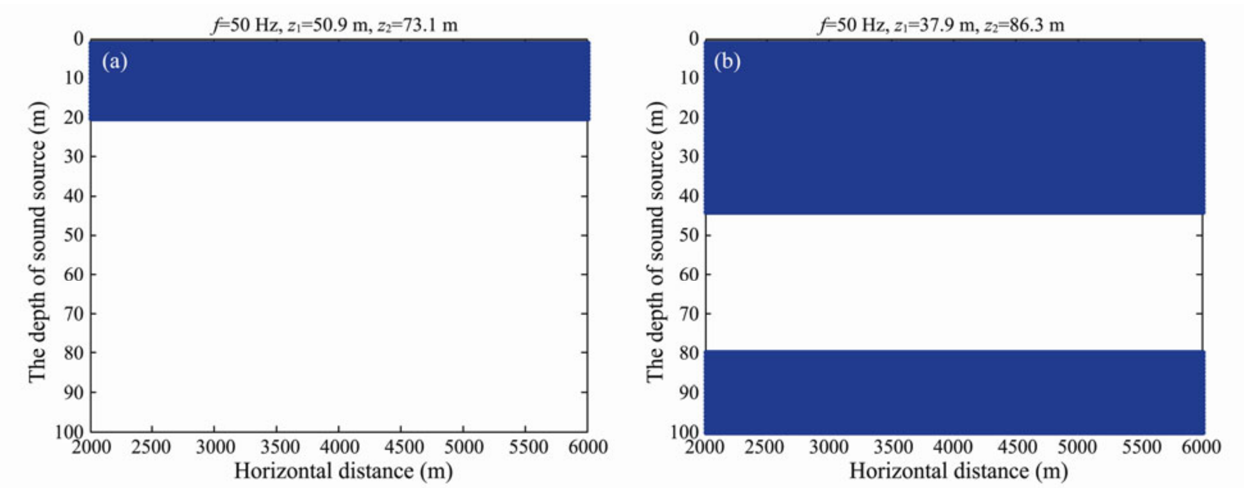

Fig.3 The sign change of ACCSPPHV with f=50 Hz.

3) The target frequency is 60 Hz. On the basis of Eqs. (18)–(19), setting h_1=20 m as the first critical surface, z_1=50.21 m and z_2=73.00 m can be obtained. If the vertical double hydrophones are placed at z_1=49.3 m and z_2=70.9 m, respectively, the summation of placing depths is 120.2 m. Fig.4(a) shows the results by Eq. (9) and Fig.4(b) by placing the vertical double hydrophones at z_1=30 m and z_2=90.6 m with the placing depth summation of 120.6 m.

With the critical surfaces of h_1=46 m and h_2=74 m, the summation of h_1 and h_2 is 120 m. All the three summations well match the corresponding theoretical effective water depth of 123.22 m.

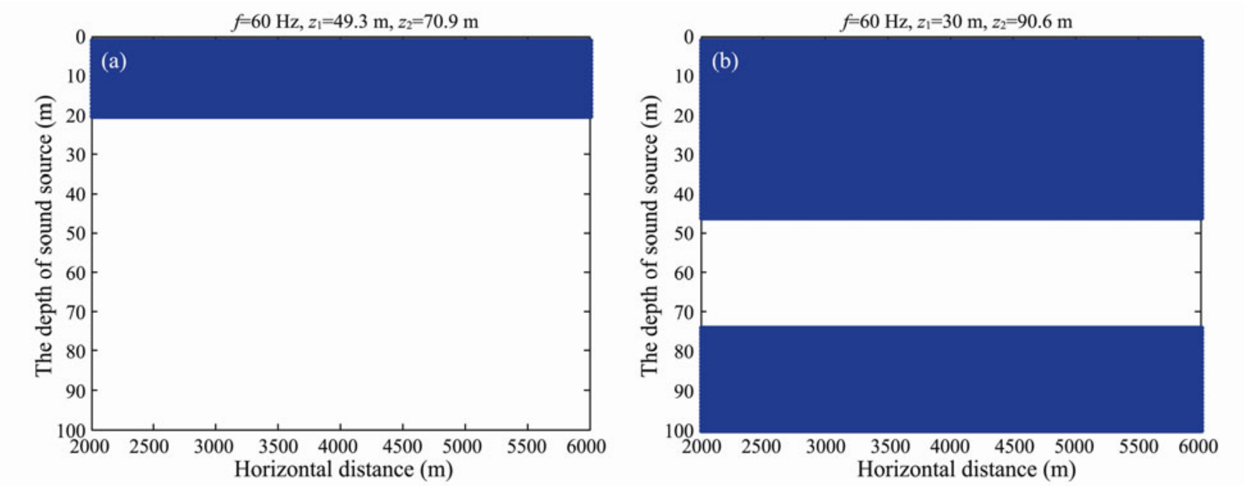

Fig.4 The sign change of ACCSPPHV with *f*= 60 Hz.

According to the above simulations at 40 Hz, 50 Hz, and 60 Hz, the effectiveness of this algorithm is proved, and some relevant conclusions can be drawn. Placing depths of the vertical double vector hydrophones can be predicted through Eqs. (18)–(19). There are errors between the predicted and actual placing positions, but they become smaller with the increase of the target frequency. The summation of the placing depths of hydrophones and that of the first and the second critical surfaces approximately equal the corresponding effective water depth, which verifies Eqs. (14) and (17).

4 Forecasting Performance Analysis

Taking the same sea environment as above, the placing position comparisons of prediction and simulation with the target frequencies of 40 Hz, 50 Hz, and 60 Hz are shown in Fig.5. In the figure the horizontal axis is the first critical surface from 10 m to 40 m with an interval of 5 m, and the vertical axis represents the placing depth of hydrophones. The results show that the forecasting performance is improved with the increase of the sound source frequency.

The summation deviations comparisons of simulation placing and placing prediction with varying frequencies of sound sources are shown in Fig.6.

From Fig.6, a conclusion can be drawn that with the increase of sound source frequencies, the summation deviations of simulation placing and placing prediction decreases. Moreover, with the increase of the critical surface h_1, the summation deviations show a decreasing trend.

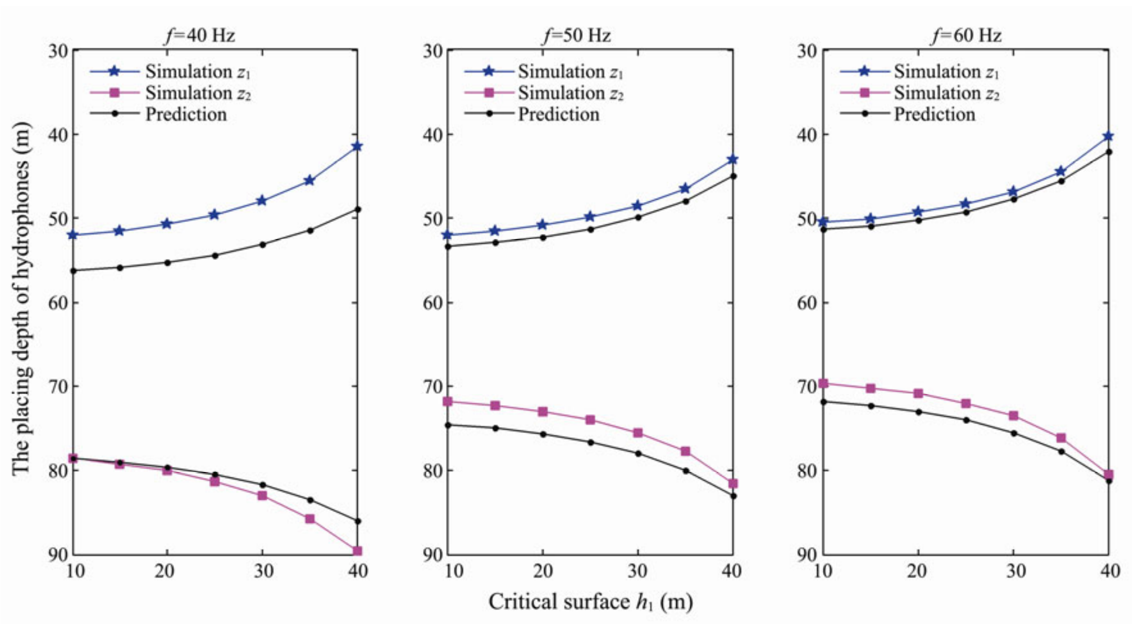

Fig.5 The placing position comparisons of prediction and simulation.

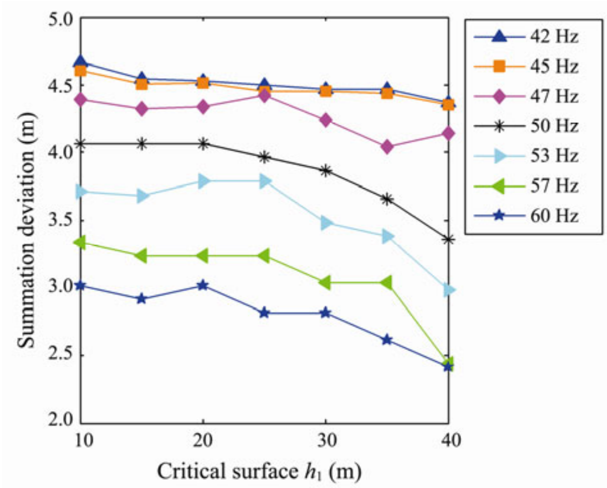

Fig.6 The summation deviations comparisons of simulation placing and placing prediction.

5 Conclusions

Based on ACCSPPHV of vertical double vector hydrophones, the depth classification algorithm of underwater targets is proposed to distinguish a surface vessel and an underwater target in this paper. Forecasting equations for placing depths are obtained when the summation of the two critical surfaces and that of placing depths equal effective water depth. The simulation and forecasting performance analysis are carried out, which verifies the effectiveness and correctness of this algorithm. In addition, this algorithm is simple and easy to implement, and has the potential for future applications in vertical arrays.

Acknowledgements

This study was supported by Public Science and Technology Research Funds Projects of Ocean (201405036-4), the National Natural Science Foundation of China (Grant Nos. 11404406, 51179034, 41072176 and 11204109), Defense Technology Research (JSJC2013604C012), and Postdoctoral Science Foundation of China (Grant No. 2013M531015).

References

Baggenstoss, P. M., 2011. An algorithm for the localization of multiple interfering sperm whales using multi-sensor time difference of arrival. *Journal of Acoustical Society of America*, **130** (1): 102-112.

Brekhovskikh, L. M., and Lysanov, Y. P., 2003. *Fundamentals of Ocean Acoustics*. Third edition. AIP Press, America, 51.

Buchingham, M. J., and Giddens, E. M., 2006. On the acoustic field in a Pekeris waveguide with attenuation in the bottom half-space. *Journal of Acoustical Society of America*, **119** (1): 123-142.

Dubreuil, M., Delrot, P., and Leonard, I., 2013. Exploring underwater target detection by imaging polarimetry and correlation techniques. *Applied Optics*, **52** (5): 997-1005.

Diamant, R., Tan, H. P., and Lampe, L., 2014. LOS and NLOS classification for underwater acoustic localization. *IEEE Transactions on Mobile Computing*, **13** (2): 311-323.

Dosso, S. E., and Wilmut, M. J., 2011. Bayesian multiple-source localization in an uncertain ocean environment. *Journal of Acoustical Society of America*, **129** (6): 3577-3589.

Forero, P. A., 2014. Broadband underwater source localization via multitask learning. *IEEE Information Sciences and Systems Conference*. Princeton, New Jersey, 1-6.

Gerstein, E. R., and Gerstein, L., 2014. Manatee hearing and sound localization can help navigate noisy shallow waters and cocktail events, no Lombard's needed. *Journal of Acoustical Society of America*, **135** (4): 2172.

Hui, J. Y., Sun, G. C., and Zhao, A. B., 2008. Normal mode acoustic intensity flux in Pekeris waveguide and its cross spectra signal processing. *Acta Acustica*, **33** (4): 300-304 (in Chinese with English abstract).

Josso, N. F., Ioana, C., Mars, J. I., and Gervaise, C., 2010. Source motion detection, estimation, and compensation for underwater acoustics inversion by wideband ambiguity lag-Doppler filtering. *Journal of Acoustical Society of America*, **128** (6): 3416-3425.

Liu, B. S., 2010. *Underwater Acoustic Principle*. Second edition. Harbin Engineering University Press, Harbin, 75 (in Chinese).

Michalopoulou, Z. H., Yardim, C., and Gerstoft, P., 2011. Particle filtering for passive fathometer tracking. *JASA Express Letters*, 1-7.

Wiggins, S. M., McDonald, M. A., and Hildebrand, J. A., 2012. Beaked whale and dolphin tracking using a multichannel autonomous acoustic recorder. *Journal of Acoustical Society of America*, **131** (1): 156-163.

Yu, Y., Hui, J. Y., and Zhao, A. B., 2008. Complex acoustic intensity and application of normal modes in Pekeris waveguide. *Acta Physic Sinica*, **57** (9): 5742-5748 (in Chinese).

Yu, Y., Hui, J. Y., and Chen, Y., 2009. Research on target depth sorting of shallow and low-frequency acoustic field. *Acta Physic Sinica*, **58** (9): 6335-6343 (in Chinese).

(Edited by Xie Jun)